Agricultural and Environmental Chemistry

Design, Synthesis and Antifungal Evaluation of Neocryptolepine Derivatives against Phytopathogenic Fungi

jiakai zhu, jian mei gao, cheng jie yang, Xiao-Fei Shang, zhong min zhao, Raymond Kobla Lawoe, rui zhou, yu sun, xiaodan Yin, and Ying-Qian Liu

J. Agric. Food Chem., **Just Accepted Manuscript** • DOI: 10.1021/acs.jafc.9b06793 • Publication Date (Web): 29 Jan 2020

Design, Synthesis and Antifungal Evaluation of Neocryptolepine Derivatives against Phytopathogenic Fungi

Jia-Kai Zhu, Jian-Mei Gao, Cheng-Jie Yang, Xiao-Fei Shang, Zhong-Min Zhao, Raymond Kobla Lawoe, Rui Zhou, Yu Sun, Xiao-Dan Yin, Ying-Qian Liu*

School of Pharmacy, Lanzhou University, Lanzhou 730000, People's Republic of China

E-mail address: yqliu@lzu.edu.cn. (Ying-qian Liu)

ABSTRACT:

Neocryptolepine is an alkaloid isolated from traditional African herbal medicine *Cryptolepis sanguinolenta* and its broad spectrum of biological activities have been illuminated in past decades. In this study, neocryptolepine and its derivatives (**1**-**49**) were designed and synthesized from economical and readily available starting materials. Their structures were confirmed by ^{1}H NMR, ^{13}C NMR and MS. The synthesized compounds were screened for their antifungal profile against six agriculturally important fungi *Rhizoctonia solani*, *Botrytis cinerea*, *Fusarium graminearum*, *Mycosphaerlla melonis*, *Sclerotinia sclerotiorum* and *Magnaporthe oryzae*. The results of *in vitro* assay revealed that compounds **5**, **21**, **24**, **35**, **40**, **45** and **47** presented remarkable antifungal activity against the fungi tested with EC_{50} values lower than 1 μg/mL. Significantly, compound **24** displayed the most effective inhibitory potency against *Botrytis cinerea* (EC_{50} = 0.07 μg/mL), and the data from *in vivo* experiments revealed that compound **24** demonstrated comparable protective activity with the positive control boscalid. Preliminary mechanism studies indicated that compound **24** showed impressive spore germination inhibitory effectiveness, lower cytotoxicity than azoxystrobin, imparted on normal function of cell membrane, cell wall and arrested the normal function of the nucleus. Besides, the excellent inhibitory activity against agriculturally important phytopathogenic fungi tested, the designed assemblage possesses several benefits with a high-profile of variation in synthesized molecules, the ease of synthesis and good cost-effectiveness of commercially available synthetic reagents, all of these have highlighted the potential

worth of compound **24** as a new and highly efficient agricultural fungicide.

KEYWORDS: Neocryptolepine, alkaloid, antifungal activity, *Botrytis cinerea.*

INTRODUCTION

The agricultural challenge of providing adequate and safe food supply for all populations is currently threatened due to infestation of food crops by virulent pathogens, especially fungi.[1,2] Crop plants have become the source of nutrients for phytopathogens at different stages of their development since the dawn of agriculture, causing a huge loss in economic value of crops thereby compromising global food security.[3] The great discoveries and developments of efficient agrochemicals to combat these pathogens have steadily succumbed to multi-drug resistance, which rendered these chemical agents ineffective.[4] Additionally, emerging results from recent investigations have indicated that resistant pathogenic species are multiplying rapidly within a short time once resistance sets in, giving rise to a new challenge to address.[5] Aside from the problems put forth, potential harm these chemical fungicides pose to human health, animals, non-target species and the environment has stirred serious concerns.[6] These concerns have continued to drive the design and synthesis of bioactive chemical agents with high efficiency, de novo modes of action, greater selectivity, biocompatibility and benign to human health as better alternatives to traditional synthetic fungicides.[7]

In this context, natural products have emerged as highly promising sources of lead candidates for use in small-molecule drug discovery.[8] It has been shown that essential features of natural products are chemical diversity and diversity in biological functions, making natural product libraries favorable and attractive in drug discovery.[9] Nonetheless, the paucity of these biologically active products in native plants and the

challenges of extracting the target compounds from other metabolites with similar chemical properties have hindered research interests in this area.[10] These problems have necessitated chemical mimicking of natural products by synthesizing libraries of structurally simplified natural compounds with improved bioactivities by adopting simple and ecofriendly synthetic protocols. Since alkaloids are biologically active compounds and play a vital role in plant defense mechanisms, alkaloids and their derivatives have often been evaluated and developed as fungicides in the past several years.[11] In the course of our previous screening for novel naturally occurring phytopesticides from the plants, neocryptolepine, a naturally isomeric indoloquinoline alkaloid, was found to exhibit superior broad-spectrum antifungal activity compared with its corresponding analogues cryptolepine and isocryptolepine,.[12] This encouraging results prompted us to further extend our investigation by synthesizing a series of new neocryptolepine derivatives and structure activity relationships on target compounds for antifungal activity were probed.(Figure 1).

Neocryptolepine is a minor alkaloid isolated from the root bark extract of traditional African herbal medicine *Cryptolepis sanguinolenta,*[13] which has been used to treat rheumatism, urinary, respiratory infections, fevers due to malaria and stomach disorders.[14] Extensive literature review has revealed the inhibitory activity of neocryptolepine against Gram-positive bacteria and Gram-negative bacteria,[15] and its antiplasmodial activity has also been extensively investigated.[16] The pioneering works of Laurent D. et al. indicated that neocryptolepine intercalated with DNA and interfered with the catalytic activity of human topoisomerase II.[17] Subsequent

111 investigations on cytotoxicity and cell cycle effects of neocryptolepine were well
112 documented.[18] Introduction of methyl group at the C11 position of neocryptolepine by
113 DIMIQ strongly enhanced the antitumor potential of this metabolite.[19] Also,
114 modification at C2 and C9 positions further improved the antitumor activity.[20,21] In
115 addition, derivatives of neocryptolepine bearing C11-alkylamino-substitution were
116 extensively evaluated to possess remarkable biological profiles against fungi, bacteria,
117 malaria and tumors.[22-26]

118 To our knowledge, there is no report on applications of neocryptolepine or its
119 derivatives against agricultural pathogens. Given the broad pharmacological activities
120 of neocryptolepine, we envisioned that chemically mimicked analogues of this plant
121 metabolite may effectively suppress activities of phytopathogenic fungi. With the
122 resurgence in multi-drug resistance, the development of more potent and
123 biocompatible neocryptolepine derivatives should yield novel antifungal agents to
124 selectively combat fungal pathogens. Hence, as continuation of our screening
125 campaign for bioactive agents against phytopathogens, a library of novel
126 neocryptolepine derivatives was designed and synthesized by employing an efficient
127 and flexible route under mild condition (Figure 2).[27] The impacts of SAR (Structure−
128 Activity Relationship) of A and D rings substitutions on inhibitory activity against six
129 phytopathogenic fungi were assessed. Compounds found to be most effective in *in*
130 *vitro* were further subjected to *in vivo* investigations. The possible mechanism action
131 of the most active compound **24** against *B. cinerea*, was preliminarily explored in this
132 study.

MATERIALS AND METHODS

Chemicals. All reagents and solvents were commercially obtained and used directly without further purification. Quinolines and indoles were purchased from a commercial source (Shanghai Sun Chemical Technology Co.,LTD).

Instruments. The melting points were determined in an open capillary using WRS-2U melting point apparatus (Shanghai Precision Instrument Co., Ltd., Shanghai, China) and are uncorrected. Mass spectra were recorded on a Bruker Daltonics APEXII49e spectrometer (Bruker Daltonics Inc., Billerica, MA, US.) with ESI source as ionization. ^{1}H and ^{13}C-NMR spectra were recorded at 400 MHz and 100 MHz on a Bruker AM-400 (Bruker Company, Billerica, MA, US.) spectrometer using TMS as reference. Microscopic morphology of fungal hyphae was observed by a Scanning electron microscopy (Hitachi, S-3400N, Japan). Microscopic internal structure of fungal cells was investigated by a transmission electron microscopy (FEI Tecnai G2 spirit Bio-Twin (T12)). The relative conductivity of hyphae was performed by a conductivity meter (Leici DDS-307, China). The absorbance of cytotoxicity assay was measured with Thermo Scientific Multiskan MK3 microplate reader (USA).

Fungi. Six plant pathogenic fungi species, *R. solani, B. cinerea, F. graminearum, M. melonis, S. sclerotiorum* and *M. oryzae* were isolated from susceptible plants cultivated in greenhouses and orchards at the Gansu academy of agricultural sciences in 2010, Gansu Province of China. Then, they were purified and identified by the Institute of Plant Protection, Gansu Academy of Agricultural Science. The fungi were maintained during the experiments on potato dextrose agar medium (PDA: potato 200

155 g, dextrose 20 g, agar 15 g and distilled water 1000 mL) at 25 °C.

156 **Synthetic Procedures.**

157 *General Synthetic Procedure for the Intermediates* ***Ⅰ***. Under nitrogen, a mixture
158 of appropriate quinoline (7.7 mmol) and MeI (11.6 mmol) in isopropanol (1 M) was
159 heated at 90 °C for 3 h. The reaction was cooled to room temperature, and the
160 resulting precipitate was isolated by vacuum filtration, washed with a mixture of
161 isopropanol/ethyl acetate (1:1), dried in vacuo, and obtained yellow solid for the next
162 step.

163 *General Synthetic Procedure for the Intermediates* ***Ⅱ***. To a solution of
164 potassium hydroxide (0.148 mol) in water (30 mL) and 1,2-dichloroethane (30 mL),
165 then the mixture was added hydrogen peroxide (6.4 mL, 35%) and
166 1-methylquinolinium iodide (**Ⅰ** , 15 mmol in 15 mL water) over 30 min at 0°C. The
167 resulting mixture was stirred at room temperature for 48 h, then the organic layer was
168 separated and the aqueous layer was extracted with dichloromethane (30 mL × 3). The
169 combined organic layer was dried with anhydrous magnesium sulfate. The organic
170 layer was concentrated under reduced pressure to obtain the title compound as a
171 yellow oil for the next step.

172 *General Synthetic Procedure for the Target Compounds* ***1-49***. A mixture of
173 Intermediate **Ⅱ** (5 mmol), indole (5 mmol) and p-TSA (5 mmol) in absolute ethanol
174 (10 mL) was stirred open to air in a 50 mL round bottom flask at reflux for 12 h. After
175 cooling to room temperature, the reaction mixture was washed with 1 M NaOH (50
176 mL) and the aqueous layer extracted with CH_2Cl_2 (3 × 80 mL). The combined organic

177 layer was then dried with anhydrous magnesium sulfate. The organic layer was
178 concentrated under reduced pressure, and the residue was purified by column
179 chromatography on silica gel, removing impurities with petroleum ether/ethyl acetate
180 (2:1), then eluting with dichloromethane/methanol (40:1) to yield the final compound
181 as a red solid.

182 The physical data of all compounds in detail are provided in Supporting
183 Information.

184 **Antifungal Activity Assay *In Vitro***

185 Neocryptolepine and its derivatives were evaluated by the mycelium growth rate
186 method[28] for their antifungal activity against six fungi, including *R. solani, B. cinerea,*
187 *F. graminearum, M. melonis, S. sclerotiorum* and *M. oryzae*. All the synthetic
188 compounds were dissolved in dimethyl sulfoxide (DMSO) and then were added to
189 potato dextrose agar (PDA) medium that was prepared and sterilized to obtain a series
190 of concentrations (50, 25, 10, 5, 2.5, 1, 0.5, 0.1, 0.05 μg/mL). The blank control was
191 maintained with 0.5% DMSO (v/v) mixed with PDA and azoxystrobin was used as a
192 positive control because azoxystrobin possesses a broad - spectrum activity against
193 phytopathogenic fungi. The mycelial disk (5mm) of phytopathogenic fungi were
194 inoculated on PDA plates and then were incubated at 25 ℃ in the dark. Each sample
195 was measured in triplicate, and its diameters (mm) of inhibition zones were measured
196 by the cross-bracketing method. The growth inhibition rates were calculated when the
197 blank control hyphae grew to the edge of the petri dish according to the following
198 formula:

199 Mycelial growth inhibition (%) = [(C − T)/(C − 5 mm)] × 100

200 Where C and T represent the diameter of fungal growth on untreated PDA and treated
201 PDA, respectively.

202 **Antifungal Activity Assay *In Vivo***

203 The protective activity *in vivo*. Based on the preceding test of *in vitro* antifungal
204 activity, compounds **5** and **24** against *B. cinerea* were further tested *in vivo* on tomato.
205 The synthesized compounds and positive control boscalid, in 0.1 mL of DMSO were
206 dissolved in 10 mL deionized water at a series of concentrations (200, 100, 50, 25
207 μg/mL). Boscalid was used as positive control because it is a specific commercial
208 fungicide for controlling *B. cinerea*. Each sample measured in quadruplicate was
209 sprayed evenly onto the tomato, which had been already washed and treated with
210 water and 75% aqueous ethyl alcohol. After 24 h, each tomato was punctured with an
211 inoculating needle and then pathogen was inoculated. 1% DMSO in 10 mL water was
212 set up as the blank control. All the treated samples were then placed into an
213 illumination incubator in 25 ℃ and 100% relative humidity for 4 days.

214 **Scanning Electron Microscopy (SEM) Observations**

215 Mycelia blocks (5.0mm×4.0 mm) were cut from the fungi after treating **24** at a
216 concentration of 0.1 μg/mL, all the samples were treated by 4% glutaraldehyde for 4 h
217 and washed three times with 0.01 M PBS (pH=7.2), then fixed with 1% osmium
218 tetraoxide solution (w/v) for 2 h. After that, each sample was dehydrated with graded
219 ethanol series (20%, 50%, 80%, 90%) for 10 min, respectively. Subsequently, the
220 samples were dried at a critical point and gold-sprayed and observed by using a

scanning electron microscope.

Transmission Electron Microscopy (TEM) Observations

The dehydrated mycelial blocks were embedded in resin at 70 °C for 24 h and then cut into thin sections. After the samples were double-stained with uranyl acetate and lead citrate, they were observed with a transmission electron microscope.

Spore Germination Inhibition Assay

Spore suspensions (1×10^5–5×10^5 spores/mL) were prepared by inoculating conidia in sterile water. The synthesized compound **24** dissolved in DMSO was added to the spore suspension at three concentrations (5, 2.5, 1 μg/mL). After that, 100 μL of the mixtures were put on concave slides and incubated in a biochemical incubator at 27 ℃, respectively. Conidial suspension with 0.5% DMSO (v/v) in water was treated as a blank control. After incubation for 12 h, the number of germinated spores were measured by approximately counting 100 conidia in blood counting chamber under a biological microscope photographic system at 400× magnification.

Determination of Cell Membrane Permeability

According to the described method,[29] the influence of candidate compound on the cell membrane relative permeability rate of *B. cinerea* was determined. The mycelial disk of *B. cinerea* (5 mm) was placed in 60 mL of PD broth medium and shaking at 140 rpm for 4 days at 27 °C. After that, the mycelia were filtered and added into the solution of **24** with different concentrations (10, 5, 1, 0.1 μg/mL, respectively). Eventually, the conductivity values were determined with a conductivity detector (at 0 h was marked as L0, and 0.5 h, 1 h, 2 h, 4 h, 6 h, 8 h, 10 h,

12 h and 24 h were marked as L1). The conductivities of samples treated by boiling water for 30 min were remarked as L2. The relative permeability rate of the cell membrane was calculated by the following formula:

Relative electric conductivity (%) = [(L1 − L0)/(L2 − L0)] × 100

Cytotoxicity of Compound 24 against Two Human Cell Lines

Cytotoxicity of target compound **24** was examined *in vitro* against two human cell lines (HL7702 and PC12) respectively following previously published procedure.[12] The cell lines tested were treated with different concentrations (25, 10, 5, 1 μg/mL respectively) of target compound **24** in the growth medium for 24 h, and the absorbance was measured at 450 nm. Five replicates were performed.

Statistical Analysis

All assays were at least performed in triplicate by conventional methods, and results were presented as means ± standard deviations. The statistical analysis was carried out by SPSS 24.0. The EC_{50} values were obtained from the parameters in the regression curves, and 95% CI, regression equation and R^2 are provided in Supporting Information.

RESULTS AND DISCUSSION

Chemistry

According to the previous work by Matthew K.V. et al.,[30] neocryptolepine derivatives were prepared using neocryptolepine as a precursor and employing an efficient and flexible method under mild conditions that provided the desired products with high yields. The detailed synthetic protocol for the preparation of

neocryptolepine and its analogues was illustrated in Figure 2. Intermediate Ⅰ was easily obtained with high yield (＞90 %) by the reaction of corresponding quinoline and methyl iodide in IPA under inert gas. Subjecting Intermediate Ⅰ to hydrogen peroxide oxidation in the mixture of potassium hydroxide aqueous solution and 1,2-dichloroethane afforded the intermediate Ⅱ without further purification. Neocryptolepine (**1**) and its analogues were produced when intermediate Ⅱ and substituted indoles were refluxed in ethyl alcohol under the catalysis of p-Toluenesulfonic acid. It is worth noting that the raw materials were obtained commercially to synthesize the intermediates and the final products with good yield. The structures of target compounds were confirmed by ^{1}H and ^{13}C NMR and MS.

***In Vitro* Activity and Structure Activity Relationship (SAR)**

An efficient and simple method was used to produce the target compounds for investigation of effects of substitutions at rings A and D of the lead compound **1** on the structure-activity relationship, wherein hydrogen at position C11, methyl at position C5 and nitrogen at position C6 were not substituted (Figure 1). All the synthesized compounds (**1-49**) and the positive control azoxystrobin were screened against six agriculturally important phytopathogenic fungi, *R. solani*, *B. cinerea*, *F. graminearum*, *M. melonis*, *S. sclerotiorum* and *M. oryzae*.

Rings A and D of the lead conpound **1** were modified to synthesize a series of novel compounds to investigate the impact of substitutions on antifungal activity against the fungi tested. And the results of inhibition rates at 10 μg/mL of all compounds indicated that some synthetic compounds possessed significant activities

with 80% higher inhibition against all six phytopathogenic fungi (Supporting Information). As shown in Tables 1 and 2, *in vitro* antifungal assay revealed that most of the tested compounds showed broad-spectrum inhibitory activity against the plant fungal pathogens tested with the EC_{50} values ranging from 1.07 to > 30 μg/mL against *Sclerotinia sclerotiorum*, 0.75 - >30 μg/mL against *Rhizoctonia solani*, 0.94 - >30 μg/mL against *Fusarium graminearum,* 0.07 - >30 μg/mL against *Botrytis cinerea* (*B. cinerea*), 0.62 - >30 μg/mL against *Magnaporthe oryzae* and 0.11 - >30 μg/mL against *Mycosphaerlla melonis*. The results indicated that most of the target compounds demonstrated bioactivity more potent than the lead compound **1,** and positive control azoxystrobin against fungi tested. Particularly, target compounds **5**, **21**, **24**, **35**, **40**, **45** and **47** were the most potent and exhibited remarkable antifungal activity against the fungi tested with EC_{50} values lower than 1 μg/mL. Notably, compounds **5** and **24** displayed the best inhibitory potency against *B. cinerea* with EC_{50} values of 0.08 μg/mL and 0.07 μg/mL respectively (Figure 3), which were superior to EC_{50} value of 4.44 μg/mL of the lead compound **1** and the EC_{50} value of ＞30μg/mL of positive control azoxystrobin. Tested compound **24** was also the most effective against *M. melonis* with EC_{50} value of 0.11 μg/mL compared to the EC_{50} value of 20.40 μg/mL of the positive control azoxystrobin. Therefore, the effect of substituents on the phenyl rings A and D was further explored. With the exception of compound **13**, compounds **4-6**, **9-11** and **15** containing electron withdrawing (Cl, F and Br) groups on the benzyl ring-A and no substituents (R_1= H) on phenyl ring-D, and compounds **19-20**, **23-25**, **28-30** and **32-33** containing electron withdrawing (Cl,

F and Br) groups on the phenyl ring-D with no substituents on the ring-A (R=H) displayed pronounced inhibitory activity against the fungi tested compared to the lead compound **1** and standard azoxystrobin.

Similarly, substitutions at the ring-A and ring-D with electron donating (CH_3 and OCH_3) groups enhanced biological profile of the tested compounds **2**-**3**, **7**-**8**, **14**, **21**-**22** and **26**-**27** against *B. cinerea and M. melonis*, respectively. The bioassay data indicated that electronic effect played a crucial role in the activity. The impact of structural variations due to the substitution pattern of the phenyl ring was also assessed. Results of activity tests showed the positioning and kind of functionality on the parent structure **1** was indispensable in antifungal activity of the synthesized compounds. Substituents at positions C2, C3, C8 and C9 were the most beneficial, providing the strongest antifungal activity (compounds **4**-**6**, **10**-**11**, **18**-**25** and **35**-**49**) against *B. cinerea* and *M. melonis* than substituents in the other positions C1, C4, C7 and C10 (compounds **12**-**15**, **26**-**27** and **30**-**33**). Additionally, the effects of the same functional group at different positions on the ring-A and ring-D were evaluated. For example, substitution of methoxy group at position 8 improved suppressive activity of the title compound **22** (EC_{50} = 0.11 μg/mL) against *B. cinerea* than substitution of methoxy group at positions 2 and 9 of the title compounds **3** (EC_{50} = 0.20 μg/mL) and **17** (EC_{50} = 0.76 μg/mL), respectively. Also, compounds **21**-**22** and **24** showed that substitution at the position 8 dominates in terms of biological effects. Replacement of 8-F by 8-Br was well tolerated with marginal loss in potency. This influence was further emphasized in substituent 8-Cl proving to be the most tolerated and active

compound than 1-Cl, 2-Cl, 3-Cl and 9-Cl, respectively. This new finding that activity was retained or improved by substitution at the 8-position gave scope for further structural modification and SAR development.

As substitution at the 8-position had given the most potent compound, the tolerances to substitution at this position were examined in detail by synthesizing novel compounds decorated with different functional groups on benzyl rings A and D to explore structural variations and effects of conformational rigidification on the antifungal activity of compounds (**34-49**) in this series as summarized in Table 3. These experimental data in general indicated that a variety of small groups were tolerated in these regions and enhanced fungicidal activity of the target compounds with EC_{50} values less than l μg/mL which were much lower than the EC_{50} values of the lead compound **1** and the positive control azoxystrobin. The extent to which functionality is tolerated was dependent on the electronic effects of the functional groups, with Cl at position 2 and Br at position 8 significantly heightened the fungicidal activity of compound **47** against *B. cinerea* with EC_{50} value of 0.09 μg/mL. Similarly, Cl at position 2 and F at position 8 improved the biological effects of compound **45** against *M. melonis with* EC_{50} value of 0.18 μg/mL. Besides, being the most potent compound *in vitro*, good solubility of compound **24** in organic solvent and water propelled it as a candidate compound.

On the other hand, most of the final products showed excellent potency against *S. sclerotiorum* and substitution at position 8 (**21**, **22**, **23**, **24**, **25**) markedly favored antifungal activity, especially compound **21** (EC_{50} = 1.07 μg/mL). Inhibitory effects

353 improved in the order: Me- < Cl- < Br- < F- < MeO- (**21**, **24**, **25**, **23** and **22**).

354 Surprisingly, most substitutions were not favorable for bioactivity against *R.*
355 *solani* with EC_{50} > 30 μg/mL compared with lead compound **1.** The unsatisfactory
356 inhibitory potential of these derivatives might be due to a different internal
357 mechanism of action exhibited against *R. solani*. This notwithstanding, title
358 compound **45** (2-Cl-8-F) was very effective against against *R. solani with* EC_{50} value
359 of 0.75 μg/mL.

360 In comparison of the bioactivity of **34**, **36-39**, **41-44**, **46-49** (with substituents on
361 ring-D), the antifungal activity of compounds **2**, **5** and **6** against *M. oryzae* with EC_{50}
362 values of 0.81, 0.63 and 0.82 μg/mL, respectively, was significantly enhanced after
363 introducing weak electron donating (CH_3) group and electron withdrawing (Cl and
364 Br) groups into position 2 of ring-A, suggesting that appreciable bioactivity could be
365 achieved through introducing substituents at position 2. Nonetheless, compounds **35**,
366 **40** and **45** with substituents on rings A and D demonstrated antifungal effects
367 comparable with compound **5**. Meanwhile, this study also offered a strategy to
368 achieve high-efficient fungicides via manipulating the positions of substituents on the
369 various rings of neocryptolepine.

370 ***In Vivo* Activity**

371 Based on the bioassay data of SAR *in vitro*, compounds **5** and **24** had been
372 chosen to further investigate their *in vivo* activity against *B. cinerea* using boscalid as
373 a positive control and 1% DMSO in 10 mL as a blank control. As presented in Figure
374 4, it was observed that the growth of hyphae was disrupted after treatment with the

target compounds compared with the blank control. The inhibitory rates of compounds **24, 5** and the positive control to boscalid were 54.91%, 32.45% and 54.61% respectively at concentration of 100 μg/mL. These results revealed that compound **24** exhibited inhibitory activity similar to the positive control boscalid and superior to compound **5**. And more significantly, this result further demonstrated the fungicidal potency of compound **24** in crop protection.

Preliminary antifungal mechanism of compound 24 against *B. cinerea*

*SEM of Compound **24** on the Hyphae Morphology*. To elucidate the effective pathway of candidate compound **24** against *B. cinerea,* the SEM had been treated with compound **24** at concentration of 0.1 μg/mL to observe the effect of compound **24** on mycelium morphology. As shown in Figure 5, in the blank control group, the hyphae grew normally and endosome of the cell appeared orderly arranged with a complete shape and a smooth surface. In contrast, after treating the SEM with compound **24**, drastic changes in mycelial morphology was observed as mycelial growth appeared abnormal, the arrangement of the endosome appeared distorted, the surface shrunk and became rough.

*TEM of Compound **24** on the Hyphae Morphology.* Ultrastructural changes of hyphae treated with compound **24** had been observed by using TEM. The natural conidia comprised an outer layer made of electron opaque mannoproteins and an inner layer with more electron transparent made of interconnected chitin and glucans. As presented in Figure 6, the hyphae of blank control revealed that mycelial cells were normal, cell membrane and cell wall were intact, and cytoplasmic organelles were

evenly distributed. After treating the TRM with compound **24**, the ultractructure of the fungus was drastically altered, the internal organelles of the cells ruptured and became disordered. Besides, the outer layer of the cell wall became detached from the cell membrane compared with blank control. This phenomenon indicated that compound **24** altered the structure of the cell wall, thereby disrupting the permeability of the cell membrane. These data indicated the shrinkage of the cell membrane was due to compound **24** and had therefore imparted the nuclear enlargement.

*Effect of Compound **24** on the Spore Germination Inhibition*. The results of spore germination inhibition assay showed that compound **24** markedly suppressed spore germination of *B. cinerea* at four different concentrations as showed in Figure 7. The data of this experiment indicated that the effect of compound **24** on the spore germination of *B. cinerea* was concentration-dependent and completely inhibited spore germination at concentration of 5 μg/mL. The position of the electron withdrawing (Cl) group on the ring-D might be the reason for the pronounced activity compound **24** *in vitro* and *in vivo* against *B. cinerea*.

*Effect of Compound **24** on the Cell Membrane Integrity*. To verify the conclusion of TEM about cell membrane integrity, the cell membrane permeability of *B. cinerea* was determined by testing the change in relative electric conductivity of mycelia suspensions with four different concentrations (10, 5, 1, 0.1 μg/mL) of compound **24**. As shown in Figure 8, the conductivity rates of the mycelia suspensions treated with compound **24** were all higher than blank control group and respectively increased in time-dependent and dose-dependent manners. Although the conductivity was

observed to be increasing, the difference between the treatment group and the blank group at each concentration was too small to elucidate that compound **24** damaged the integrity of the cell membrane. Therefore, it was reasoned that candidate compound **24** slightly affected the cell membrane as the concentrations increased, but this was not the effect of the excellent *in vitro* activity of compound **24** against *B. cinerea*.

Cytotoxicity Assay

Synthesized compound **24** was probed for cytotoxicity against two human cell lines HL7702 and PC12 cell lines *in vitro* by employing azoxystrobin as a positive control. As shown in Figure 9, the results indicated that compound **24** displayed lower cytotoxicity compared to positive control azoxystrobin against the two cell lines tested at different concentrations (25, 10, 5, 1 μg/mL respectively). It is noteworthy that when the concentration reached 25 μg/mL, compound **24** was equipotent to azoxystrobin against PC12. Compared with the excellent antifungal activity *in vitro* and *in vivo*, cytotoxicity of compound **24** was not significant.

In summary, neocryptolepine had been used as a lead structure to design and synthesize a series of novel bioactive derivatives with respect to structure and chemical diversity. The synthesized compounds were screened for their antifungal profile against six important phytopathogenic fungi. This study demonstrated that substitutions at C2 of ring A and C8 of ring D of the lead compound **1** played a key role to improve susceptibilities of the fungi tested to the final target compounds. Moreover, the results of *in vitro* bioassay demonstrated that compounds **5**, **21**, **24**, **35**, **40**, **45** and **47** exhibited pronounced antifungal activity compared with

441 neocryptolepine, and compound **24,** in particular, was found to possess the best
442 activity with EC_{50} value of 0.07 μg/mL against *B. cinerea*. The data from *in vivo*
443 experiment also showed that compound **24** demonstrated protective performance
444 comparable to the positive control boscalid. Additionally, the observations of SEM
445 and TEM indicated that compound **24** caused a slight damage to the cell membrane,
446 imparted the cell wall of fungus and arrested the normal function of the cell nucleus.
447 Furthermore, compound **24** completely inhibited the spore germination at
448 concentration of 5 μg/mL, and displayed lower cytotoxicity than azoxystrobin against
449 HL7702 and PC12 cell lines *in vitro* at different concentrations. Compound **24**,
450 therefore, displayed great potency to be used as highly efficient antifungal agent
451 because it demonstrated an excellent inhibitory effectiveness against the agriculturally
452 significant fungi tested. Besides, the effective inhibitory activity, the designed library
453 holds several merits with a high level of diversity in synthesized molecules, the ease
454 of synthesis and good cost-effectiveness of commercially available synthetic reagents.
455 Further explorations on structural modification of compound **24** and its specific
456 mechanisms of action are in progress.
457

458 **ASSOCIATED CONTENT**

459 **Supporting Information**

460 The Supporting Information is available free of charge on the ACS Publications
461 website at DOI:

462 *In vitro* antifungal activity against six phytopathogenic fungi at 10 μg/mL; *In vitro*

463 EC_{50} values of all compounds against six phytopathogenic fungi in detail; Detailed
464 data of all synthesized compounds; ^{1}H NMR, ^{13}C NMR and Mass spectra of the
465 representative compounds.

466 **Corresponding Author**

467 E-mail: yqliu@lzu.edu.cn.

468 **Notes**

469 The authors declare no competing financial interest.

470 **ACKNOWLEDGEMENTS**

471 This work was supported financially by the National Key Research and Development
472 Program of China (2017YFD0201404) and the National Natural Science Foundation
473 of China (21877056, 21672092); Support was also supplied by the Key Program for
474 international S&T cooperation projects of China Gansu Province (18YF1WA115).

475

476

477

478

479

480

481

482

483

484

REFERENCES

1. Tückmantel, S.; Greul, J. N.; Janning, P.; Brockmeyer, A.; Grütter, C.; Simard, J. R.; Gutbrod, O.; Beck, M. E.; Tietjen, K.; Rauh, D.; Schreier, P. H. Identification of Ustilago maydis Aurora Kinase As a Novel Antifungal Target. *ACS Chem. Biol.* 2011, 6 (9), 926-933.

2. Hou, Z.; Zhu, L.-F.; Yu, X.-c.; Sun, M.-Q.; Miao, F.; Zhou, L. Design, Synthesis, and Structure-Activity Relationship of New 2-Aryl-3,4-dihydro-β-carbolin-2-ium Salts as Antifungal Agents. *J. Agric. Food Chem.* 2016, 64 (14), 2847-2854.

3. Mishra, J.; Arora, N. K. Secondary metabolites of fluorescent pseudomonads in biocontrol of phytopathogens for sustainable agriculture. *Appl. Soil. Ecol.* 2018, 125, 35-45.

4. Ishii, H. Studies on fungicide resistance in phytopathogenic fungi. *J. Gen. Plant Pathol.* 2004, 70 (6), 379-381.

5. Wang, P.-Y.; Wang, M.-W.; Zeng, D.; Xiang, M.; Rao, J.-R.; Liu, Q.-Q.; Liu, L.-W.; Wu, Z.-B.; Li, Z.; Song, B.-A.; Yang, S. Rational Optimization and Action Mechanism of Novel Imidazole (or Imidazolium)-Labeled 1,3,4-Oxadiazole Thioethers as Promising Antibacterial Agents against Plant Bacterial Diseases. *J. Agric. Food Chem.* 2019, 67 (13), 3535-3545.

6. Abbaszadeh, S.; Sharifzadeh, A.; Shokri, H.; Khosravi, A. R.; Abbaszadeh, A. Antifungal efficacy of thymol, carvacrol, eugenol and menthol as alternative agents to control the growth of food-relevant fungi. *J. Mycol. Med.* 2014, 24 (2), e51-e56.

7. Zhang, J.; Liu, J.; Ma, Y.; Ren, D.; Cheng, P.; Zhao, J.; Zhang, F.; Yao, Y. One-pot

507 synthesis and antifungal activity against plant pathogens of quinazolinone derivatives
508 containing an amide moiety. *Bioorg. Med. Chem. Lett.* 2016, 26 (9), 2273-2277.
509 8. Zhigan, J.; Na, L.; Dandan, H.; Guoqiang, D.; Zhenyuan, M.; Jianzhong, Y.;
510 Haiying, H.; Yuanying, J.; Wannian, Z.; Yan, W.; Chunquan S. The discovery of
511 novel antifungal scaffolds by structural simplification of the natural product
512 sampangine. *Chem. Commun.* 2015, 51 (78), 14648.
513 9. Wang, X.; Wang, M.; Yan, J.; Chen, M.; Wang, A.; Mei, Y.; Si, W.; Yang, C.
514 Design, Synthesis and 3D-QSAR of New Quinazolin-4(3H)-one Derivatives
515 Containing a Hydrazide Moiety as Potential Fungicides. *ChemistrySelect* 2018, 3
516 (38), 10663-10669.
517 10. Ehrenworth, A. M.; Peralta-Yahya, P. Accelerating the semisynthesis of
518 alkaloid-based drugs through metabolic engineering. *Nat. Chem. Biol.* 2017, 13, 249.
519 11. Symington, S. B.; Zhang, A.; Karstens, W.; Houten, J. V.; Clark, J. M.
520 Characterization of Pyrethroid Action on Ciliary Calcium Channels in Paramecium
521 tetraurelia. *Pestic. Biochem. Phys.* 1999, 65 (3), 181-193.
522 12. Li, J.-c.; Wang, R.-x.; Sun, Y.; Zhu, J.-k.; Hu, G.-f.; Wang, Y.-l.; Zhou, R.; Zhao,
523 Z.-m.; Liu, Y.-q.; Peng, J.-w.; Yan, Y.-f.; Shang, X.-f. Design, synthesis and
524 antifungal activity evaluation of isocryptolepine derivatives. *Bioorg. Chem.* 2019, 92,
525 103266.
526 13. Cimanga, K.; Bruyne, T. D.; Pieters, L.; Claeys, M.; Vlietinck, A. J. T. L. New
527 alkaloids from Cryptolepis sanguinolenta. *Tetrahedron Lett.* 1996, 37 (10),
528 1703-1706.

529 14. Lionel, G.; Patrizia, A.; Frédéric, R.; Sabine, V. M.; Emilie, T.; Luc, P.; Valérie,
530 G.; Edwin, D. P.; Alexandre, O.; Jean-Fran Ois, R. J. B. Interactions of cryptolepine
531 and neocryptolepine with unusual DNA structures. *Biochimie* 2003, 85 (5), 535-547.
532 15. Cimanga, K.; Bruyne, T., De; Pieters, L.; Totte, J.; Tona, L.; Kambu, K.; Berghe,
533 D. V.; Vlietinck, A. J. Antibacterial and antifungal activities of neocryptolepine,
534 biscryptolepine and cryptoquindoline, alkaloids isolated from Cryptolepis
535 sanguinolenta. *Phytomedicine*. 1998, 5 (3), 209-214.
536 16. Cimanga, K., .; Bruyne, T., De; Pieters, L., .; Vlietinck, A. J.; Turger, C. A. In
537 vitro and in vivo antiplasmodial activity of cryptolepine and related alkaloids from
538 Cryptolepis sanguinolenta. *J. Nat. Prod.* 1997, 60 (7), 688.
539 17. Bailly, C.; Laine, W.; Baldeyrou, B.; De Pauw-Gillet, M. C.; Colson, P.; Houssier,
540 C.; Cimanga, K.; Van, M. S.; Vlietinck, A. J.; Pieters, L. DNA intercalation,
541 topoisomerase II inhibition and cytotoxic activity of the plant alkaloid
542 neocryptolepine. *Anti-cancer Drug Des.* 2000, 15 (3), 191-201.
543 18. Dassonneville, L.; Lansiaux, A.; Wattelet, A.; Wattez, N.; Mahieu, C.; Miert, S.
544 V.; Pieters, L.; Baillya, C. Cytotoxicity and cell cycle effects of the plant alkaloids
545 cryptolepine and neocryptolepine: relation to drug-induced apoptosis. *Eur. J.*
546 *Pharmacol.* 2000, 409 (1), 9-18.
547 19. Peczyńska-Czoch, W.; Osiadacz, J.; Kaczmarek, Ł.; Żal, T. Microbial
548 transformation of azacarbazoles X: Regioselective hydroxylation of
549 5,11-dimethyl-5H-indolo [2,3-b]quinoline, a novel DNA topoisomerase II inhibitor,
550 by Rhizopus arrhizus. *Biotechnol. Lett.* 1996, 18 (2), 123-128.

551 20. Humeniuk Rita; Kaczmarek Łukasz; ska-Czoch Wanda; Marcinkowska Ewa.
552 Cytotoxicity and cell cycle effects of novel indolo[2,3-b]quinoline derivatives. *Oncol.*
553 *Res.* 2003, 13 (5), 269-277.
554 21. Sidoryk, K.; Świtalska, M.; Wietrzyk, J.; Jaromin, A.; Piętka-Ottlik, M.; Cmoch,
555 P.; Zagrodzka, J.; Szczepek, W.; Kaczmarek, Ł.; Peczyńska-Czoch, W. Synthesis and
556 Biological Evaluation of New Amino Acid and Dipeptide Derivatives of
557 Neocryptolepine as Anticancer Agents. *J. Med. Chem.* 2012, 55 (11), 5077-5087.
558 22. El Sayed, I.; Van der Veken, P.; Steert, K.; Dhooghe, L.; Hostyn, S.; Van Baelen,
559 G.; Lemière, G.; Maes, B. U. W.; Cos, P.; Maes, L.; Joossens, J.; Haemers, A.;
560 Pieters, L.; Augustyns, K. Synthesis and Antiplasmodial Activity of
561 Aminoalkylamino-Substituted Neocryptolepine Derivatives. *J. Med. Chem.* 2009, 52
562 (9), 2979-2988.
563 23. Mei, Z.-W.; Wang, L.; Lu, W.-J.; Pang, C.-Q.; Maeda, T.; Peng, W.; Kaiser, M.;
564 El Sayed, I.; Inokuchi, T. Synthesis and in Vitro Antimalarial Testing of
565 Neocryptolepines: SAR Study for Improved Activity by Introduction and
566 Modifications of Side Chains at C2 and C11 on Indolo[2,3-b]quinolines. *J. Med.*
567 *Chem.* 2013, 56 (4), 1431-1442.
568 24. El-Gokha, A. A.; Boshta, N. M.; Hussein, M. K. A.; Sayed Ibrahim EL-T. EL.
569 Synthesis and structure-activity relationships of novel neocryptolepine derivatives.
570 *Chem. Res. Chinese U.* 2017, 33 (3), 373-377.
571 25. Sidoryk, K.; Jaromin, A.; Edward, J. A.; Świtalska, M.; Stefańska, J.; Cmoch, P.;
572 Zagrodzka, J.; Szczepek, W.; Peczyńska-Czoch, W.; Wietrzyk, J.; Kozubek, A.;

573 Zarnowski, R.; Andes, D. R.; Kaczmarek, Ł. Searching for new derivatives of
574 neocryptolepine: Synthesis, antiproliferative, antimicrobial and antifungal activities.
575 *Eur. J. Med. Chem.* 2014, 78, 304-313.
576 26. Okada, M.; Mei, Z.-W.; Imran Hossain, M.; Wang, L.; Tominaga, T.;
577 Takebayashi, T.; Murakami, M.; Yasuda, M.; Shigehiro, T.; Kasai, T.; Mizutani, A.;
578 Murakami, H.; El Sayed, I. E. T.; Dan, S.; Yamori, T.; Seno, M.; Inokuchi, T.
579 Synthesis and in vitro cancer cell growth inhibition evaluation of 11-amino-modified
580 5-Me-indolo[2,3-b]quinolines and their COMPARE analyses. *Med. Chem. Res.* 2016,
581 25 (5), 879-892.
582 27. Liu Y. -Q.; Zhu J. -K.; Li J. -C.; Ma Q.; Yang G. -Z.; Zhao Z. -M.; Peng J. -W.;
583 Feng J. -X. Application of A ring-modified new cryptolepine derivatives in
584 prevention and control of agricultural plant diseases, CN 109717198.
585 28. Rashid, T. S.; Awla, H. K.; Sijam, K. Antifungal effects of Rhus coriaria L. fruit
586 extracts against tomato anthracnose caused by Colletotrichum acutatum. *Ind. Crop*
587 *Prod.* 2018, 113, 391-397.
588 29. Gao, Y.; He, L.; Li, X.; Lin, J.; Mu, W.; Liu, F. Toxicity and biochemical action
589 of the antibiotic fungicide tetramycin on Colletotrichum scovillei. *Pestic. Biochem.*
590 *Phys.* 2018, 147, 51-58.
591 30.Vecchione, M. K.; Sun, A. X.; Seidel D. Divergent reactions of indoles with
592 aminobenzaldehydes: indole ring-opening vs. annulation and facile synthesis of
593 neocryptolepine. *Chem. Sci.* 2011, 2 (11), 2178.
594

595

596 **Figure Captions**

597 **Figure 1**. Strategy of Neocryptolepine derivatives as potent antifungal agents.

598 **Figure 2**. Synthetic route of Neocryptolepine and its derivatives.

599 **Figure 3.** *In vitro* antifungal activities of compound 24 against *B. cinerea*.

600 **Figure 4.** *In vivo* protective antifungal activities of candidate compounds against *B.*
601 *cinerea*.

602 **Figure 5.** Scanning electron micrographs of the hyphae from the colony of *B. cinerea*.

603 **Figure 6.** Transmission electron microscopy observations of cell structure of *B.*
604 *cinerea*. Ultrastructure of the hyphae in the untreated control (A and B), treated with
605 compound 24 at concention of 0.1 μg/mL(C and D).

606 **Figure 7.** Spore germination inhibition assays of compound 24 against *B. cinerea*.

607 **Figure 8.** Determination of cell membrane permeability of compound 24 against *B.*
608 *cinerea*.

609 **Figure 9.** Cytotoxicity assay of compound 24 against cell lines HL7702 and PC12.

610

611

612

613

614

615

616

617

	EC_{50} (μg/mL)					
compound	*S.s.*	*R.s.*	*B.c.*	*F.g.*	*M.o.*	*M.m.*
1	17.65	9.00	4.44	16.31	17.63	1.16
2	4.01	8.92	0.21	1.83	0.81	1.77
3	3.72	7.11	0.20	2.77	1.30	0.78
4	6.21	> 30	0.23	13.95	17.37	1.87
5	5.03	11.79	0.08	0.94	0.63	0.98
6	2.96	> 30	0.10	3.77	0.82	0.98
7	6.59	8.76	0.55	5.31	8.54	1.01
8	6.01	> 30	0.54	12.82	11.41	2.22
9	> 30	12.93	0.92	16.79	17.98	2.17
10	3.16	6.68	0.20	8.47	10.19	0.88
11	3.97	> 30	0.27	20.87	10.02	1.56
12	> 30	> 30	1.78	22.34	20.41	7.29
13	15.59	19.29	> 30	22.67	15.90	7.39
14	12.98	13.48	0.72	8.27	6.07	2.91
15	> 30	> 30	4.13	> 30	16.57	4.32
azoxystrobin	> 30	> 30	> 30	27.43	12.03	20.40

618 **Table 1**. Antifungal Activity of A Ring Substitution Compounds *in Vitro.*

619 *S.s., Sclerotinia sclerotiorum ; R.s., Rhizoctonia solani; B.c., Botrytis cinerea; F.g., Fusarium*
620 *graminearum; M.o., Magnaporthe oryzae; M.m., Mycosphaerlla melonis.* All values are the mean
621 of three replicates.

622

623

624

625

626

compound	EC_{50} (μg/mL)					
	S.s.	*R.s.*	*B.c.*	*F.g.*	*M.o.*	*M.m.*
16	3.70	12.87	0.28	4.86	3.24	1.36
17	6.10	13.79	0.76	5.70	5.92	3.31
18	8.98	14.04	0.29	8.75	18.73	2.01
19	4.26	13.48	0.78	5.24	4.96	1.17
20	5.04	> 30	0.90	1.88	2.06	1.63
21	1.07	14.04	0.09	2.80	3.14	0.83
22	5.77	> 30	0.11	8.63	5.20	1.16
23	4.03	3.52	0.13	6.62	11.96	0.14
24	2.80	4.93	0.07	1.92	2.82	0.11
25	2.90	5.45	0.12	6.00	5.09	0.14
26	10.67	> 30	2.41	9.44	12.67	4.06
27	> 30	> 30	3.92	18.65	> 30	7.60
28	5.41	> 30	5.00	> 30	> 30	2.12
29	12.49	> 30	8.67	> 30	9.71	0.78
30	14.42	> 30	> 30	> 30	> 30	0.45
31	> 30	> 30	5.19	> 30	> 30	11.71
32	> 30	> 30	> 30	> 30	> 30	> 30
33	> 30	> 30	> 30	> 30	> 30	> 30
azoxystrobin	> 30	> 30	> 30	27.43	12.03	20.40

627 **Table 2**. Antifungal Activity of D Ring Substitution Compounds *in Vitro.*

628 *S.s., Sclerotinia sclerotiorum ; R.s., Rhizoctonia solani; B.c., Botrytis cinerea; F.g., Fusarium*
629 *graminearum; M.o., Magnaporthe oryzae; M.m., Mycosphaerlla melonis.* All values are the mean
630 of three replicates.

631

632

633

634

compound	EC_{50} (μg/mL)					
	S.s.	*R.s.*	*B.c.*	*F.g.*	*M.o.*	*M.m.*
34	> 30	> 30	3.93	> 30	> 30	2.58
35	1.93	5.29	0.16	1.63	0.64	0.43
36	2.97	> 30	0.16	1.72	0.97	0.50
37	4.21	> 30	0.28	2.82	1.05	0.75
38	4.74	> 30	0.49	3.46	1.19	0.96
39	5.87	> 30	0.42	4.22	1.84	0.77
40	2.68	5.36	0.14	1.48	0.62	0.30
41	3.62	> 30	0.21	1.79	0.69	0.24
42	4.08	> 30	0.13	1.19	0.83	0.50
43	3.83	> 30	0.17	2.05	0.79	0.52
44	4.87	> 30	0.19	2.82	1.10	0.71
45	2.77	0.75	0.10	6.51	0.62	0.18
46	5.16	> 30	0.11	9.49	6.55	0.28
47	8.44	> 30	0.09	19.50	10.59	1.22
48	3.52	> 30	0.17	1.22	0.94	0.64
49	5.98	> 30	0.23	6.36	0.78	0.87
azoxystrobin	> 30	> 30	> 30	27.43	12.03	20.40

635 **Table 3**. Antifungal Activity of A and D Rings Substitution Compounds *in Vitro*.

636 *S.s., Sclerotinia sclerotiorum ; R.s., Rhizoctonia solani; B.c., Botrytis cinerea; F.g., Fusarium*

637 *graminearum; M.o., Magnaporthe oryzae; M.m., Mycosphaerlla melonis*. All values are the mean

638 of three replicates.

639

640

641

642

643

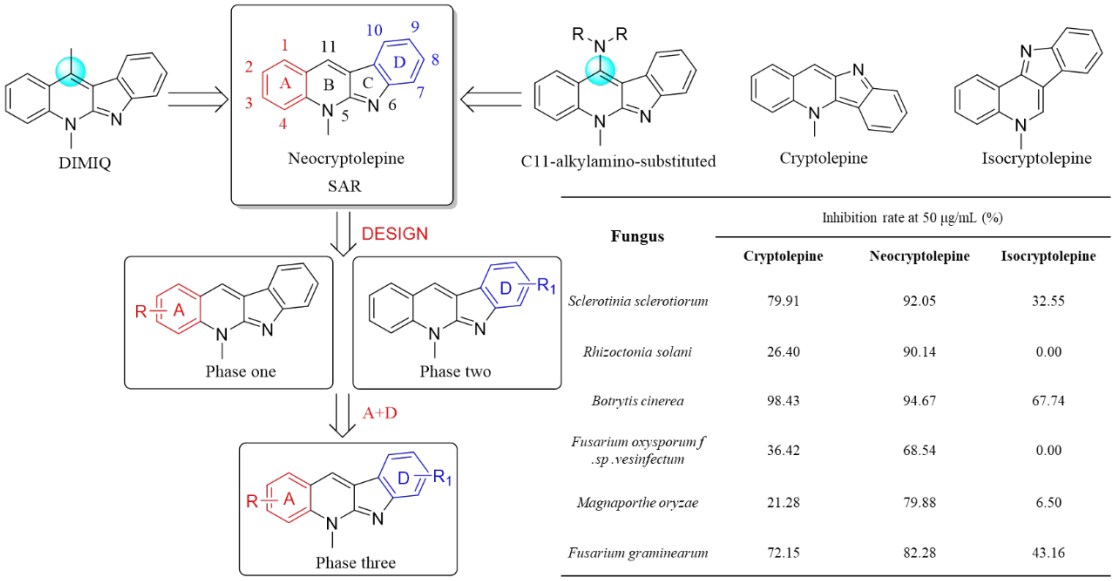

Fungus	Inhibition rate at 50 μg/mL (%)		
	Cryptolepine	Neocryptolepine	Isocryptolepine
Sclerotinia sclerotiorum	79.91	92.05	32.55
Rhizoctonia solani	26.40	90.14	0.00
Botrytis cinerea	98.43	94.67	67.74
Fusarium oxysporum f .sp .vesinfectum	36.42	68.54	0.00
Magnaporthe oryzae	21.28	79.88	6.50
Fusarium graminearum	72.15	82.28	43.16

644

645 **Figure 1**. Strategy of Neocryptolepine derivatives as potent antifungal agents.

646

647

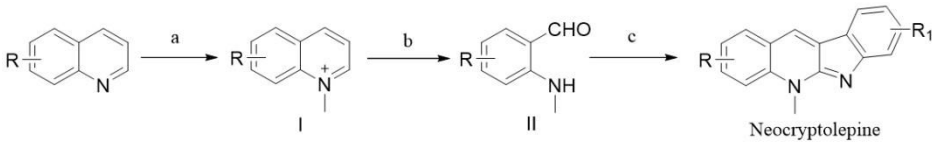

Reagents and conditions: (a) IPA, CH_3I, 3 h; (b) KOH, H_2O_2, 48 h; (c) indole, p-TSA, EtOH, 24 h.

Compound	R	R_1	Compound	R	R_1	Compound	R	R_1
1	H	H	18	H	9-F	35	2-OCH_3	8-F
2	2-CH_3	H	19	H	9-Cl	36	2-OCH_3	8-Cl
3	2-OCH_3	H	20	H	9-Br	37	2-OCH_3	8-Br
4	2-F	H	21	H	8-CH_3	38	2-OCH_3	8-CH_3
5	2-Cl	H	22	H	8-OCH_3	39	2-OCH_3	8-OCH_3
6	2-Br	H	23	H	8-F	40	2-CH_3	8-F
7	3-CH_3	H	24	H	8-Cl	41	2-CH_3	8-Cl
8	3-OCH_3	H	25	H	8-Br	42	2-CH_3	8-Br
9	3-F	H	26	H	10-CH_3	43	2-CH_3	8-CH_3
10	3-Cl	H	27	H	10-OCH_3	44	2-CH_3	8-OCH_3
11	3-Br	H	28	H	10-F	45	2-Cl	8-F
12	4-CH_3	H	29	H	10-Cl	46	2-Cl	8-Cl
13	4-F	H	30	H	10-Br	47	2-Cl	8-Br
14	1-CH_3	H	31	H	7-CH_3	48	2-Cl	8-CH_3
15	1-Cl	H	32	H	7-Cl	49	2-Cl	8-OCH_3
16	H	9-CH_3	33	H	7-Br			
17	H	9-OCH_3	34	2-OCH_3	9-OCH_3			

648

649 **Figure 2**. Synthetic route of Neocryptolepine and its derivatives.

650

651

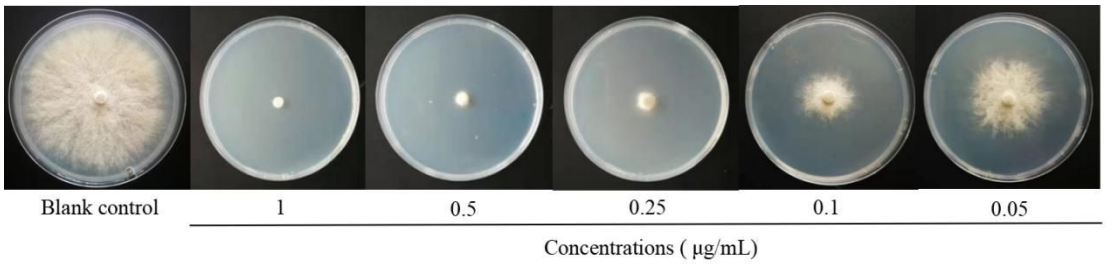

652

653 **Figure 3**. *In vitro* antifungal activities of compound 24 against *B. cinerea.*

654

655

656

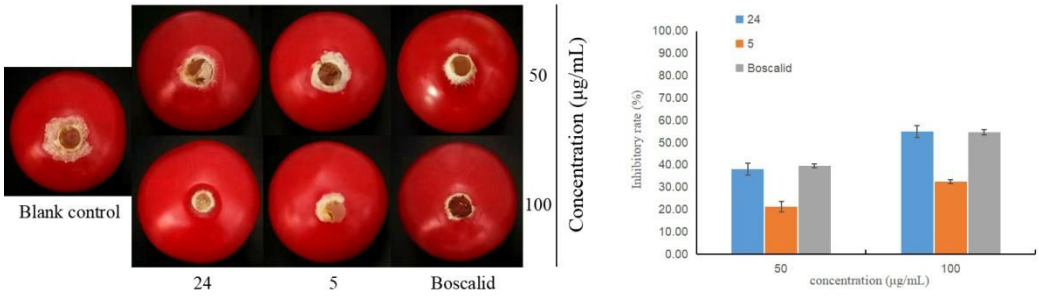

657

658 **Figure 4**. *In vivo* protective antifungal activities of candidate compounds against *B.*

659 *cinerea*.

660

661

662

663

664

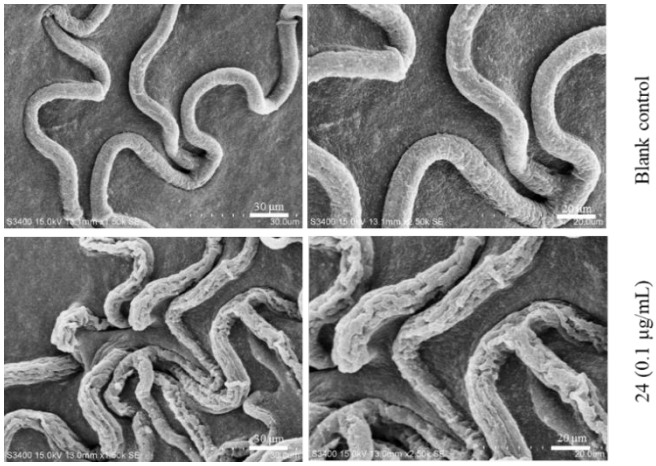

665

666 **Figure 5**. Scanning electron micrographs of the hyphae from the colony of *B. cinerea*.

667

668

669

670

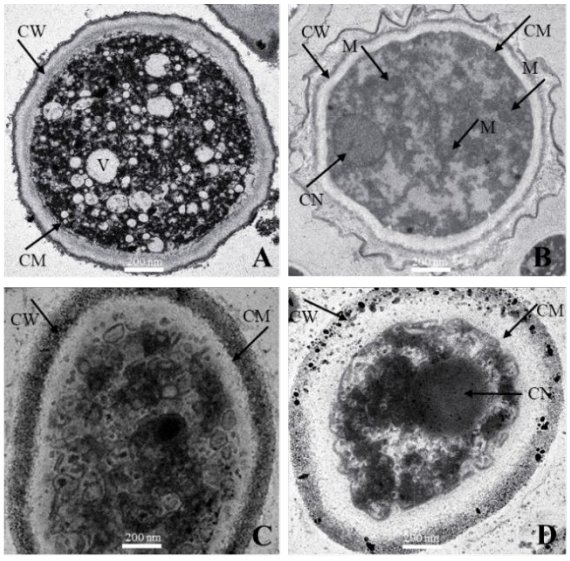

671

672 **Figure 6**. Transmission electron microscopy observations of cell structure of *B.*

673 *cinerea*. Ultrastructure of the hyphae in the untreated control (A and B), treated with

674 compound 24 at concention of 0.1 μg/mL(C and D). Cell wall (CW); cell nucleus

675 (CN); vacuole (V) and mitochondria (M); After treatment, the organelles were

676 severely damaged, and cell nucleus were significantly enlarged.

677

678

679

680

681

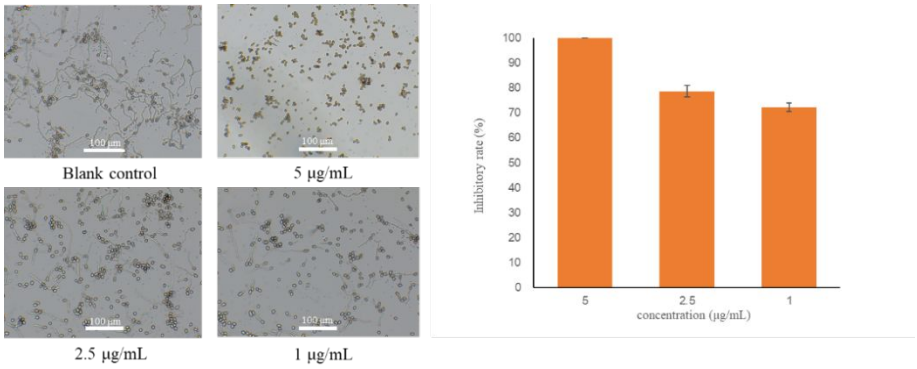

682

683 **Figure 7**. Spore germination inhibition assays of compound 24 against *B. cinerea*.

684

685

686

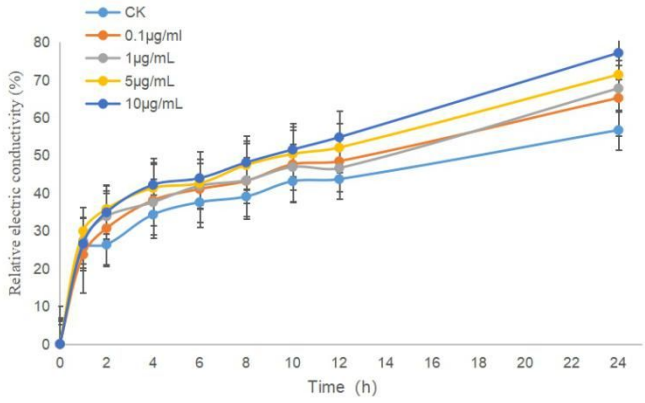

687

688 **Figure 8**. Determination of cell membrane permeability of compound 24 against *B.*

689 *cinerea.*

690

691

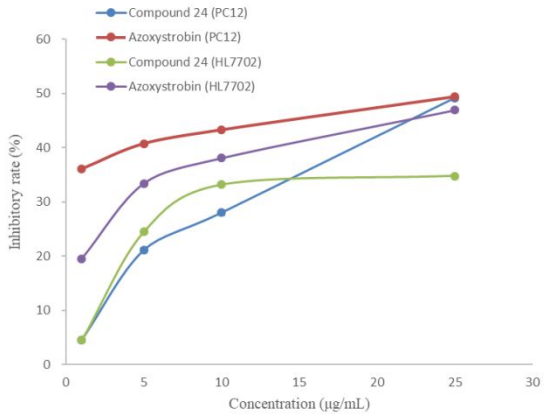

692

693 **Figure 9.** Cytotoxicity assay of compound **24** against cell lines HL7702 and PC12.

694

695

696

697

698

699

700

701

702

703

704

705

706

707

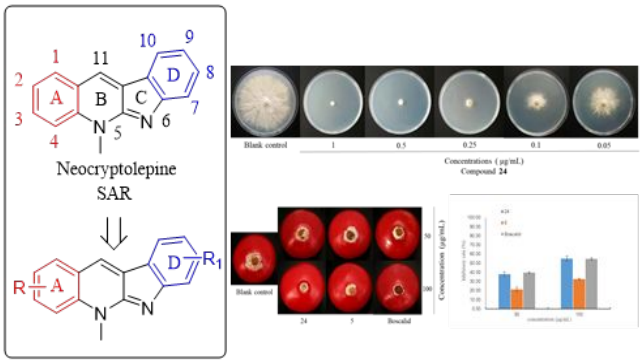

Graphical abstract